Sustained delivery of sphingosine-1-phosphate using poly(lactic-co-glycolic acid)-based microparticles stimulates Akt/ERK-eNOS mediated angiogenesis and vascular maturation restoring blood flow in ischemic limbs of mice

Sustained delivery of sphingosine-1-phosphate using poly(lactic-co-glycolic acid)-based microparticles stimulates Akt/ERK-eNOS mediated angiogenesis and vascular maturation restoring blood flow in ischemic limbs of mice

Xun Qi[a,b], Yasuo Okamoto[a], Tomomi Murakawa[c], Fei Wang[a], Osamu Oyama[a], Ryunosuke Ohkawa[d], Kazuaki Yoshioka[a], Wa Du[a], Naotoshi Sugimoto[a], Yutaka Yatomi[d], Noriko Takuwa[a,e], and Yoh Takuwa[a,*]

[a]*Department of Physiology, Kanazawa University Graduate School of Medicine, 13-1 Takara-machi, Kanazawa, Ishikawa 920-8640, Japan.* [b]*Department of Pharmacology, Pharmaceutical College of China Medical University, Beier Road 92, Heping District, Shenyang, Liaoning Province 110001, P. R. China.* [c]*JST Innovation Plaza Ishikawa, 2-13 Asahidai, Noumi, Ishikawa 923-1211, Japan.* [d]*Department of Clinical Laboratory Medicine, The University of Tokyo Graduate School of Medicine, 7-3-1 Hongo, Bunkyo-ku, Tokyo 113-0033, Japan.* [e]*Department of Health and Medical Sciences, Ishikawa Prefectural Nursing University, 7-1 Nakanuma-tu, Kahoku, Ishikawa 929-1212, Japan*

***Corresponding author:** Yoh Takuwa, M.D., Ph.D., Department of Physiology, Kanazawa University Graduate School of Medicine, 13-1 Takara-machi, Kanazawa 920-8640, Japan.

Phone: +81-76-265-2167 Fax: +81-76-234-4223

E-mail: ytakuwa@med.kanazawa-u.ac.jp

Abstract

Therapeutic angiogenesis is a promising strategy for treating ischemia. The lysophospholipid mediator sphingosine-1-phosphate (S1P) acts on vascular endothelial cells to stimulate migration and tube formation, and plays the critical role in developmental angiogenesis. We developed poly(lactic-co-glycolic-acid) (PLGA)-based S1P-containing microparticles (PLGA-S1P), which are biodegradable and continuously release S1P, and studied the effects of PLGA-S1P on neovascularization in murine ischemic hindlimbs. Intramuscular injections of PLGA-S1P stimulated blood flow in C57BL/6 mice dose-dependently, with repeated administrations at a 3-day interval, rather than a single bolus or 6-day interval, over 28 days conferring the optimal stimulating effect. In Balb/c mice that exhibit limb necrosis and dysfunction due to retarded blood flow recovery, injections of PLGA-S1P stimulated blood flow with alleviation of limb necrosis and dysfunction. PLGA-S1P alone did not induce edema in ischemic limbs, and rather blocked vascular endothelial growth factor-induced edema. PLGA-S1P not only increased the microvessel densities in ischemic muscle, but promoted coverage of vessels with smooth muscle cells and pericytes, thus stabilizing vessels. PLGA-S1P stimulated Akt and ERK with increased phosphorylation of endothelial nitric oxide synthase in ischemic muscle. The effects of the nitric oxide synthase inhibitor, Nω-nitro-L-arginine methylester, showed that PLGA-S1P-induced blood flow stimulation was partially dependent on nitric oxide. Injections of PLGA-S1P also increased the expression of

angiogenic factors and the recruitment of CD45-, CD11b- and Gr-1-positive myeloid cells, which are implicated in post-ischemic angiogenesis, into ischemic muscle. These results indicate that PLGA-based, sustained local delivery of S1P is a potentially useful therapeutic modality for stimulating post-ischemic angiogenesis.

Keywords: sphingosine-1-phosphate, poly(lactic-co-glycolic acid), sustained release, angiogenesis, ischemia

1. Introduction

Therapeutic angiogenesis is an attractive strategy for treating patients with ischemia (Ferrara and Kerbel, 2005; Losordo and Dimmeler, 2004a). To date, the therapeutic efficacy of angiogenic peptide growth factors, including vascular endothelial growth factor (VEGF) and fibroblast growth factor-2 (FGF-2), and their expression plasmids, has been tested with their topical and systemic administration (Ferrara and Kerbel, 2005; Losordo and Dimmeler, 2004a; Simons, 2005). However, the trials failed to show unequivocal efficacy of the tested agents partly due to insufficient gene transduction or rapid washout of proteins. High local concentrations of angiogenic factors increase the risks including edema and atherosclerosis. A controlled drug delivery system for sustained release of angiogenic factors would be more favorable for therapeutic angiogenesis (Simons, 2005).

Sphingosine-1-phosphate (S1P) is a lipid mediator that exerts pleiotropic effects mainly via G-protein-coupled receptors, $S1P_1$, $S1P_2$, and $S1P_3$ (Ishii et al., 2004; Kluk and Hla, 2002; Morris et al., 2009; Takuwa et al., 2008). Vascular endothelial cells (ECs) largely express $S1P_1$ and $S1P_3$, which stimulate EC proliferation, migration, and capillary-like tube formation *in vitro* (Kimura et al., 2000; Lee et al., 1999; Ryu et al., 2002; Wang et al., 1999). S1P also maintains endothelial barrier function via $S1P_1$ (Lee et al, 2006; Peng et al., 2004; Singleton et al., 2005). S1P stimulated angiogenesis *in vivo* via $S1P_1$ and $S1P_3$ in Matrigel plugs implanted in mice (Lee et al., 1999). Deletion of the genes of $S1P_1$ and the S1P-synthesizing

enzymes sphingosine kinases-1 and -2 in mice resulted in defects in vascular maturation, i.e. recruitment process of pericytes and smooth muscle cells to nascent capillaries, in developmental angiogenesis (Allende et al., 2003; Liu et al., 2000; Mizugishi et al., 2005). The S1P-$S1P_1$ axis is involved in tumor neovascularization (Chae et al., 2004; Visentin et al., 2006). Thus, the S1P signaling pathway is a key regulator in angiogenesis under physiological and pathophysiological conditions.

Recently, we demonstrated for the first time that daily intramuscular injections of S1P solutions promoted blood flow in murine ischemic hindlimbs (Oyama et al., 2008). The stimulatory effect on the blood flow of an optimal dose of S1P was similar or a little stronger in magnitude as that induced by FGF-2. S1P-induced stimulation of blood flow was accompanied by an increase in the capillary density. However, since daily injections of a therapeutic agent do not seem to be favorable in clinical setting, development of sustained release formulation of S1P would be desirable.

Microspheres made from poly(lactic-co-glycolic acid) (PLGA) are biocompatible and bioabsorbable (Crotts and Park, 1998), and have been successfully employed as a controlled drug delivery system for sustained release of various drugs (Allison, 2008). In the present study, we have developed new sustained release preparations of S1P by using PLGA-based microparticles (PLGA-S1P). We explored usefulness of topically applied PLGA-S1P microparticles. We show here that intermittent repeated local injections of PLGA-S1P into

ischemic limb muscle promoted blood flow recovery with stimulation of microvessel formation and vascular maturation without adverse effects including tissue edema. These effects involved Akt/ERK-endothelial nitric oxide synthase (eNOS) activation.

2. Materials and Methods

2.1. Materials

DL-erythro-sphingosine-1-phosphate (S1P) was bought from BIOMOL (Plymouth Meeting, PA). Nω-nitro-L-arginine methylester (L-NAME), fatty acid-free bovine serum albumin (BSA), and poly(vinyl alcohol) were purchased from Sigma (St. Louis, MO). PLGAs were purchased from Wako Pure Chemical Industries (Osaka, Japan). Recombinant mouse $VEGF_{164}$ and pentobarbital were purchased from R&D systems (Minneapolis, MN) and Kyoritsu (Tokyo, Japan), respectively.

2.2. Animals

We used C57BL/6J and Balb/c male mice of 8–12 week old (Nippon SLC, Shizuoka, Japan). In hindlimb ischemia model due to femoral arteriectomy (see 2. 4.), Balb/c mice show retarded recovery of blood flow compared with C57BL/6J mice and consequently exhibit limb necrosis and functional impairments due to tissue ischemia unlike C57BL/6J mice

(Helisch et al., 2006; Shireman and Quinines, 2005). Therefore, we employed C57BL/6J mice to determine the effects of PLGA-S1P and L-NAME on angiogenesis, blood flow, cellular signaling, and gene expression in most experiments of the present study (Fig. 1, 3-8), and Balb/c mice to see its preventive effects on limb necrosis and functional impairments (Fig. 2). Green fluorescent protein (GFP)-transgenic (Tg) mice were kindly donated by Dr. Masaru Okabe at Osaka University. Mice were housed in a temperature-controlled conventional facility (24 °C) under a 12:12 h light–dark cycle with free access to regular chow and water. All experiments using mice were approved by and performed according to the Guidelines for the Care and Use of Laboratory Animals in Kanazawa University, which strictly conforms to US National Institutes of Health guidelines.

2.3. Preparation of PLGA-S1P microparticles

PLGA-S1P microparticles were prepared by a previously reported emulsion solvent diffusion method in water (Kawashima et al., 1998). In brief, 60 mg of either of four different PLGAs (PLGA5005 (lactide/glycolide (L/G) molar ratio of 50:50 and average molecular weight (MW) of 5,000), PLGA5010 (L/G ratio of 50:50 and MW of 10,000), PLGA7505 (L/G ratio of 75:25 and MW of 5,000), and PLGA7510 (L/G ratio of 75:25 and MW of 10,000)) and 1 mg of S1P were dissolved completely in dichloromethane (2.4 ml) and acetone (0.6 ml). The resultant organic solution was poured into 12 ml of an aqueous poly(vinyl alcohol) solution

(2.5%) and stirred at room temperature overnight. The entire dispersed system was then centrifuged and resuspended in distilled water. The resultant dispersion was dried using a freeze-drying method. The encapsulated amount of S1P in PLGA-S1P microparticles was determined by dissolving PLGA-S1P microparticles in a physiological solution (Ham's F12 medium) containing 0.1% Tween 80 and measuring released amounts of S1P with high performance liquid chromatography as described previously (Ohkawa et al., 2008). The average S1P content encapsulated in PLGA-S1P microparticles was 1.2% (w/w). Analysis of the external surface morphology of the PLGA microparticles by microscopy exhibited a spherical shape with smooth and uniform surface morphology. The diameter of the final PLGA microparticles was ranged in 10-30 μm. Among the above four PLGAs tested, we found that PLGA5005 exhibited most stable release profile *in vitro* by continuously monitoring amounts of S1P released into a solution when S1P-containing PLGA microparticles were incubated in the physiological solution: the average amounts of S1P released from three different batches of PLGA5005-S1P (1 mg of the initial amount) into 1 ml of the physiological solution were 6.56±1.94 (mean±S.E.M) nmol in 1-3 days, 3.07±0.59 nmol in 4-6 days, 1.13±0.18 nmol in 7-9 days, 0.82±0.06 nmol in 10-12 days, and 0.72±0.18 nmol in 13-15 days.

2.4. Unilateral hindlimb ischemia model of mice

Mice were subjected to surgical procedures to achieve unilateral hindlimb ischaemia after intraperitoneal injection of pentobarbital (60 mg/kg), according to the method described previously (Oyama et al., 2008). In brief, following a skin incision at the left paracenter of the lower abdomen, the femoral artery, which originated from the external iliac artery and terminated to bifurcate into the saphenous and the popliteal arteries, was exposed. The femoral artery was ligated with 8-0 silk, and the whole length of the femoral artery was excised and the skin incision sutured.

2.5. Drug administration

Microparticles of PLGA-S1P or PLGA were suspended in Dulbecco's phosphate-buffered saline (PBS) containing 0.1% fatty acid-free BSA. VEGF was dissolved in PBS, aliquoted, and stored at –30°C. It was diluted to the final concentration in PBS containing 0.1% fatty acid-free BSA. Ten microlitres each of the suspensions of either PLGA-S1P or PLGA alone with or without VEGF was injected intramuscularly into four sites in the medial portion of the thigh muscle and two sites in the calf muscle of ischemic limbs for 28 days in a single bolus or divided doses at 3 or 6 day intervals.

L-NAME, a NOS inhibitor, was dissolved in the drinking water (0.5 mg/ml) containing 1 % glucose and administered into mice for 4 weeks before and after the operation whereas control animals received drinking water containing 1 % glucose. We chose this dose of

L-NAME because it was previously shown to induce hypertension through inhibition of NO production (Obst et al., 2004). All animals were fed a regular chow diet. Systolic and diastolic blood pressure and heart rate were measured in conscious mice by the tail-cuff system using BP98A (Softron Co, Tokyo, Japan) according to manufacturer's protocol.

2.6. Laser Doppler blood flow analysis

The blood flow of ischemic (left) and contra-lateral non-ischaemic (right) hindlimbs was measured with a laser Doppler blood flow (LDBF) analyzer (Moor Instruments, Devon, UK) before and after operation. Before each measurement, mice were anaesthetized with pentobarbital (60 mg/kg, intraperitoneally injected) and placed upon a plate warmed at 37 °C for 15 min. After scanning, the stored data were analyzed to quantify the mean LDBF per unit two-dimensional area on the en-face image of each entire hindlimb in mice at the supine position, which was determined by the software provided by the manufacturer (Moor Instruments). For each animal, the values were expressed as the ratio of LDBF values in ischemic (left)/non-ischaemic control (right) limb at a given time point.

2.7. Assessment of limb necrosis and active hindlimb movement

The severity of hindlimb tissue necrosis was assessed serially at indicated time points by using the following scale; "0", no necrosis; "1", necrosis of one toe; "2", necrosis of two or

more toes; “3”, necrosis of the foot; “4”, necrosis of the leg; “5” autoamputation of the entire leg (Shireman and Quinones, 2005). The function of ischemic hindlimbs was assessed by using the scoring system based on the active foot movement; “0”, spontaneous movement of non-ischemic right hindlimbs; “1”, dragging of foot; “2”, no dragging but no active plantar flexion; “3”, moderately to severely reduced plantar flexion; “4”, normal or only mildly abnormal use (Helisch et al., 2006). Assessment of both limb necrosis and movement was performed by an observer who was blinded to treatment.

2.8. Immunohistochemistry and immunofluorescence

Mice were perfused with PBS containing 4% paraformaldehyde through a cannula inserted into left ventricle, and the calf muscle was excised, embedded in O.C.T. compound (Sakura Fine Chemical, Tokyo, Japan), and frozen on dry ice. Acetone-fixed frozen sections were incubated with rat monoclonal anti-CD31/PECAM-1 antibody (1:100, clone MEC13.3, BD Biosciences, San Jose, CA), mouse monoclonal anti-α smooth muscle actin (αSMA) (1:100, clone 1A4, Sigma), rabbit polyclonal anti-NG2 (1:200, AB5320, Chemicon), rat monoclonal anti-CD11b (1:200, BD Biosciences), rat monoclonal anti-Gr-1 (1:200, BD Biosciences) and rat monoclonal anti-CD45(1:200, BD Biosciences). For immunofluorescence, bound antibodies were detected with goat AlexaFluor 488- or 594-conjugated secondary antibodies and fluorescent images were obtained with a confocal microscope (Carl Zeiss LSM510

Pascal). CD31-positive capillary densities were counted in randomly chosen 10 high power fields per mouse and expressed as the number of capillaries per mm^2. The quantification of the extents of αSMA- and NG2-positive mural cell ensheathement of microvasculatures was carried out using Image J software (NIH). For immunohistochemistry, tissue sections probed with primary antibodies were incubated with a biotinylated anti-rat IgG antibody and streptoavidin-conjugated peroxidase (Vectastain ABC kit, Vector Laboratories, Burlingame, CA, USA), followed by visualization with 3,3'-diaminobenzidine tetrahydrochloride. The stained sections were observed with a microscope (Olympus, BX41), and the quantification of the number of CD11b-, CD45- and Gr-1-positive cells was carried out using Image J software.

2.9. Western Blotting

Excised muscle tissues were snap-frozen in liquid nitrogen and homogenated in ice-cold buffer (50 mM Tris/HCl (pH 7.2), 500 mM NaCl, 10 mM $MgCl_2$, 1% Triton X-100, 0.5% deoxycholate, 0.1% sodium dodecyl sulfate (SDS), 10 μg/ml leupeptin, 10 μg/ml aprotinin, 1 mM phenylmethanesulfonyl fluoride) by a glass homogenizer. After removal of tissue debris by centrifugation 800 g at 4 °C for 15 min, the supernatants were used for Western blot analysis. 75 μg proteins were loaded and separated on SDS-8% or 12% polyacrylamide gels and electrotransferred onto Immobilon-P membrane (Millipore, Bedford, MA), followed by

probing with rabbit polyclonal anti-Ser^{1177}-phosphorylated-eNOS antibody (1:1000, Cell Signaling, Danvers, MA), rabbit polyclonal anti-Ser^{473}-phosphorylated-AKT antibody (1:1000, Cell Signaling), rabbit polyclonal anti-Thr^{202},Tyr^{204}-phosphorylated-ERK antibody (1:1000, Cell Signaling), rabbit polyclonal anti-eNOS antibody (1:1000, Cell Signaling), rabbit polyclonal anti-Akt antibody(1:1000, Cell Signaling), rabbit polyclonal anti-ERK antibody (1:1000, Cell Signaling).

2.10. Isolation of mRNA and quantitative real-time polymerase chain reaction (PCR)

Total RNA was isolated with TRIzol® (Invitrogen, Carslbad, CA) from calf muscle. The concentration of RNA was determined by spectrophotometry at 260 nm. 1 μg of total RNA was reverse-transcribed with Rever Tra Ace (Toyobo, Osaka, Japan). Real-time quantitative PCR analysis was performed using the ABI PRISM 7300 sequence detection system (Applied Biosystems, Foster, CA). The following primers and TaqMan probes (Applied Biosystems) were used: $VEGF_{164}$ (Vegfa, ID# Mm00437308_m1), FGF-2 (Fgf2, ID# Mm00433287_m1), HGF (Hgf, ID# Mm01135185_m1), angiopoietin-1 (Angpt-1) (Angpt1, ID# Mm00456498_m1), transforming growth factor-β1 (TGF β1) (Tgfb1, ID# Mm00441726_m1), platelet-derived growth factor B (PDGF-B) (Pdgfb, ID# Mm01298578_m1), interleukin-1β (IL-1β) (Il1b, ID# Mm00434228_m1), stromal cell-derived factor-1 (SDF-1) (Cxcl12, ID# Mm00445553_m1). TaqMan Rodent Glyceraldehyde-3-phosphate Dehydrogenase (GAPDH)

Control Reagents (Applied Biosystems) were used as an endogenous control. The cycling condition was programmed as follows: activation of AmpErase uracil-*N*-glycosylase for prevention of carryover contamination at 50 °C for 2 min, activation of AmpliTaq Gold DNA polymerase at 95 °C for 10 min, 40 cycles of denaturation at 95 °C for 15 s and annealing/extension at 60 °C for 1 min. ΔCt was calculated as (gene of interest Ct) − (*GAPDH* Ct) using Sequence detector (Applied Biosystems) and Microsoft Excel (Microsoft corp., Redmond, WA, USA). The relative quantity of mRNA of gene of interest was calculated by $\Delta\Delta$Ct calculation as $2^{-((\Delta\text{Ct of treated sample})-(\Delta\text{Ct of control sample}))}$. The amplification efficiencies of the target and the endogenous reference were confirmed by observing the equal relationship between cDNA dilution and ΔCt. All experiments included negative controls consisting of no cDNA for each primer pair.

2.11. Bone marrow transplantation

The recipient mice were irradiated 1 day before bone marrow transplantation by a sublethal dosage of 9.6 Gray. Bone marrow cells were collected by flushing the marrow cavity of femurs of GFP-Tg donor mice. Unfractionated bone marrow cells (1×10^7) were injected into recipient mice via a tail vein. We analyzed GFP fluorescence in peripheral blood cells by using a fluorescence activated cell sorter (FACS, JSAN Cell sorter, Bay bioscience, Japan).

2.12. Evaluation of tissue edema using X-ray computed tomography (CT)

Mice given injections of PLGA or PLGA-S1P were subjected to X-ray computed tomography using LaTheta LCT-100 (Aloka, Tokyo, Japan) at indicated time points. The CT images of hindlimbs were acquired by cutting 8 slices every 1 mm distance from greater trochanter of femur to patella, and the volume of soft tissue except bone tissue in ischemic (left) and non-ischemic (right) limbs were calculated to evaluate the tissue edema using Image J software.

2.13. Blood cell counts, plasma collection, blood biochemistry and urine test

The abdomen of mice that were sacrificed by an overdose (2 mg) of pentobarbital was quickly opened and blood was collected into a heparinized syringe via vena cava. Plasma was derived after centrifugation (2,500 × *g*, 4°C, 15 min) and stored at −80°C. Measurement of blood cells, leukocyte fractions, blood urea nitrogen and alanine aminotransferase was determined by SRL (Hachiohji, Japan). The bladder area on the abdomen of conscious mice held by hands was gently massaged, and expelled urine was collected in a 1.5 ml microtube. Urine glucose and protein were determined by a urine test paper (Wako, Osaka, Japan).

2.14. Statistics

All values are expressed as the mean ± S.E.M. (standard error of mean). The data were

analyzed using two-way analysis of variance (ANOVA) followed by Dunnett's post-hoc test (Fig. 1) or followed by Bonfferoni post test (Fig. 3 and 7A), and one-way ANOVA followed by Bonfferoni post test (Fig. 7B) (Prism 5.0, GraphPad Software, Inc., San Diego, CA). Statistical significance between two groups was analyzed by Student's t test (Fig. 2-6 and 8). Values of $P < 0.05$ were considered statistically significant.

3. Results

3.1. Local administration of S1P-containing PLGA microparticles stimulates blood flow recovery and ameliorates necrosis and dysfunction in ischemic hindlimbs

We studied the effects of S1P-containing PLGA (PLGA-S1P) microparticles on blood flow in ischemic hindlimbs after surgical femoral arteriectomy in C57BL/6 mice. The identical total amount of PLGA-S1P microparticles was injected into ischemic limb muscle as either a single bolus or divided doses at either 3-day interval or 6-day interval for 28 days (Fig. 1A). The standard total amount (180 pmol S1P per mouse) was determined based upon our previous observations obtained with daily injections of S1P solutions (Oyama et al., 2008). Divided injections of PLGA-S1P at a 3-day interval, but not single bolus injection or divided injections at a 6-day interval, significantly enhanced the blood flow recovery compared with PLGA alone on postoperative day 14 and 28 (Fig. 1B and C). The single bolus injection and

the divided injections at a 6-day interval also tended to stimulate blood flow recovery, although statistically not significant (Fig. 1B and C). PLGA alone did not affect blood flow recovery compared with vehicle solution, indicating that PLGA microparticle alone was without any effect on blood flow recovery. We compared the effects of different doses of PLGA-S1P microparticles on blood flow. The 3-day interval injections of 1.8, 18 and 54 pmol PLGA-S1P/mouse stimulated blood flow on postoperative day 28 and other time points with the optimal effect obtained at 18 pmol (Fig. 1D). A previous study (Forrest et al., 2004) showed that systemic administration of S1P and its derivatives induced bradycardia and lymphopenia in rodents. Local injections of PLGA-S1P did not affect the body weight, blood pressure, heart rate, blood cell count including lymphocyte number, blood chemistry, and urinary glucose and protein (Table 1). For the following experiments, we took advantage of 3-day interval injections of the optimal dose.

It was previously shown that the extent and the time course of blood flow recovery and consequently the extent of limb damage due to ischemia differ in different inbred mouse strains (Helisch et al., 2006; Shireman and Quinones, 2005). For example, the Balb/c strain shows delayed and poor recovery of blood flow compared with C57BL/6 mice, and is complicated by limb tissue damage and impaired limb activity. As shown in Fig. 2A, Balb/c mice that received injections of PLGA alone had relatively low perfusion in ischemic hindlimbs compared with C57BL/6 mice (Fig. 1C). The 3-day interval injections of

PLGA-S1P significantly increased the blood flow in ischemic limbs on postoperative day 7, 21, and 28 in Balb/c mice compared with PLGA alone (Fig. 2A). PLGA-S1P significantly reduced severity of limb necrosis on postoperative day 5, 7, 10 and 28, as assessed by using a five-point scale (Shireman and Quinones, 2005) (Fig. 2B). We applied the scoring for classifying the active hindlimb movements to evaluate limb function (Helisch et al., 2006). Injections of PLGA-S1P promoted recovery of limb function at 14, 21 and 28 days (Fig. 2C). These results indicated that local injections of PLGA-S1P stimulated blood flow recovery, inhibited tissue damage, and improved the functional capacity in ischemic hindlimbs in BALB/c strain.

3.2. PLGA-S1P microparticles inhibit VEGF-induced edema in ischemic hindlimbs of C57BL/6 mice

S1P acts on vascular ECs to suppress vascular permeability via $S1P_1$ receptor *in vitro* (Lee et al., 2006; Peng et al., 2004; Singleton et al., 2005). In contrast, a potent angiogenic factor VEGF induces vascular hyperpermeability and consequently tissue edema (Ferrara and Kerbel, 2005; Losordo and Dimmeler, 2004a; Simons, 2005; Takahashi and Shibuya, 2005). We studied the effect of PLGA-S1P on VEGF-induced edema formation. Either VEGF (a total of 56 ng per mouse over 28 days) or PLGA-S1P (a total of 180 pmol per mouse) alone stimulated blood flow recovery to the similar extent (Fig. 3A). This dose of VEGF was

determined in our preliminary experiments, which showed that higher VEGF doses than the employed dose induced more severe limb edema but did not further enhance blood flow. The combination of VEGF and PLGA-S1P did not show an additive or synergistic effect on blood flow recovery. We evaluated the extent of edema in ischemic limbs by determining soft tissue volumes of hindlimbs with a microCT scanner. The limb edema, which was elicited by the surgery by itself and peaked on postoperative day 1, was similar in magnitude among the four groups of PLGA vehicle, PLGA-S1P alone, VEGF alone, and the combination of VEGF and PLGA-S1P (Fig. 3B). The edema subsided by postoperative day 5 in PLGA and PLGA-S1P groups. In contrast, in VEGF-administered mice the edema was still persistent throughout the observation period of time although the extent of edema declined after postoperative day 1 (Fig. 3C). The combination of PLGA-S1P and VEGF did not induce edema at the sustained phase, indicating that PLGA-S1P prevented VEGF-induced edema.

3.3. Local administration of PLGA-S1P microparticles stimulates neovascularization with promotion of vascular maturation in C57BL/6 mice

We studied the effects of PLGA-S1P injection on neovascularization by double immunofluorescence using anti-CD31 (EC marker) and anti-αSMA (smooth muscle marker) antibodies in C57BL/6 mice. Injections of PLGA-S1P resulted in a 30% increase in the anti-CD31 staining-positive microvessel density in calf muscle of ischemic limbs on

postoperative day 28, compared with injections of PLGA alone (Fig. 4A and 4C). Anti-αSMA-positive blood vessels were also increased in ischemic muscle of mice given PLGA-S1P injections compared with PLGA injections (Fig. 4A and 4C). The anti-αSMA-positive vascular cross-sectional area was increased in PLGA-S1P administered mice compared with PLGA (Fig. 4C), indicating that relatively larger blood vessels were formed in ischemic muscle of mice given PLGA-S1P injections. Thus, in PLGA-S1P administered mice, blood vessels paved with mural smooth muscle were better developed compared with PLGA. Double immunofluorescence using anti-CD31 and anti-NG2 (pericyte marker) antibodies showed that NG2-positive microvessels in ischemic muscle were increased in mice given PLGA-S1P injections compared with PLGA injections (Fig. 4B and 4C). These observations indicate that PLGA-S1P increases pericyte-covered capillaries and smooth muscle-paved larger vessels in ischemic muscle.

3.4. PLGA-S1P promotes blood flow recovery in a nitric oxide (NO)-dependent manner in C57BL/6 mice

We studied the mechanisms for PLGA-S1P-induced stimulation of angiogenesis and blood flow. We first explored the effects of PLGA-S1P on the mRNA expression of various angiogenic factors by real time-PCR analysis. Among the angiogenic factors examined, the mRNA expression of IL-1β, HGF, TGF- β1, SDF-1, and PDGF-B increased in ischemic limb

muscle compared with non-ischemic muscle (Fig. 5). Furthermore, injections of PLGA-S1P in ischemic muscle increased the expression of angiopoietin-1, HGF, IL-1β and SDF-1, suggesting that S1P-induced increases in the expression of these angiogenic factors might at least in part contribute to stimulated neovascularization in ischemic limbs.

We next examined the involvement of NOS in S1P-induced neovascularization in ischemic limbs. Previous *in vitro* studies showed that S1P activates Akt to stimulate eNOS through Akt-mediated phosphorylation of eNOS in vascular ECs (Igarashi et al., 2001; Nofer et al., 2004; Rikitake et al., 2002). Recently, ERK1/2 was also shown to mediate eNOS stimulation through phosphorylation of eNOS (Urano et al., 2008). Stimulation of eNOS and consequent increase in NO production contributes to stimulation of post-ischemic angiogenesis and blood flow recovery (Ferrara and Kerbel, 2005; Simons, 2005; Ziche et al., 1997). We observed that PLGA-S1P injections stimulated phosphorylation of both Akt and ERK with an increase in phosphorylation of eNOS in ischemic limb muscle (Fig. 6), suggesting that S1P stimulated eNOS probably through Akt and ERK in ischemic limb muscle *in vivo*. Systemic administration of L-NAME, a NOS inhibitor, into mice given PLGA injection profoundly inhibited blood flow recovery in ischemic limbs (Fig. 7A). L-NAME administration into mice given PLGA-S1P injections abolished PLGA-S1P induced increase in blood flow over the levels of mice given PLGA injection. We confirmed that the administration of the employed dose of L-NAME induced an increase in systolic blood

pressure (120 ± 4.6 mmHg in control mice vs. 150 ± 4.1 mmHg in L-NAME-treated mice), indicating the effectiveness of L-NAME. L-NAME administration tended to inhibit PLGA-S1P-induced increase in the microvascular density in ischemic muscle as evaluated with anti-CD31 immunohistochemistry (P=0.11, L-NAME+PLGA-S1P versus PLGA-S1P) (Fig. 7B).

3.5. PLGA-S1P mobilizes bone marrow-derived cells (BMDCs) into ischemic limb muscle in C57BL/6 mice

Previous studies (Asahara et al., 1999; Ohki et al., 2005) showed that BMDCs are recruited to ischemic sites and contribute to neovascularization in the murine hindlimb ischemic model. We studied the effect of PLGA-S1P injections on recruitment of BMDCs into ischemic limb muscle by analyzing C57BL/6 mice that had received transplantation of bone marrow from GFP-Tg mice. Peripheral blood cells of the recipients were almost completely (> 95%) reconstituted with GFP-positive cells after 5 weeks. Fluorescence microscopic observations of frozen sections of limb muscle showed that GFP-positive BMDCs infiltrating into ischemic muscle were increased in mice given PLGA-S1P injections compared with PLGA injections (Fig. 8A). GFP-positive cells were virtually not observed in non-ischemic muscle in mice. Immunohistochemical staining using antibodies against the pan-myeloid cell marker CD45, the myelomonocytic lineage cell marker anti-CD11b, and the neutrophil marker Gr-1 showed

that myeloid cells positive for these markers were infiltrating in ischemic muscle (Fig. 8B, 8C and 8D). Injections of PLGA-S1P increased BMDCs positive for either CD45, CD11b or Gr-1, indicating that S1P stimulated recruitment of BMDCs into ischemic limb muscle.

4. Discussion

Current attempts to develop therapeutic angiogenesis are categorized into the angiogenic factor therapy to supply angiogenic growth factors by either their direct administration or gene transduction of the expression vectors and the cell therapy to supply bone marrow-derived vascular precursor cells and/or angiogenic molecules-producing cells. In the previous approaches of direct administration of the angiogenic factors, one of the major limitations was thought to be the short tissue half-life of the angiogenic proteins. One approach to overcome this problem would be to employ slow release formulations of angiogenic factors. In the present study, we developed a slow release formulation of the lipid angiogenic factor S1P by using PLGA as a drug-delivery system. We showed here that repeated, local injections of PLGA-S1P microspheres at a regular interval are effective in stimulating blood flow in ischemic limbs and improving ischemia-induced limb necrosis and impaired function without the side effects including tissue edema and bradycardia. These beneficial effects of PLGA-S1P are achieved by increases in both microvessels and smooth

muscle-covered larger vessels in ischemic limb muscle. In addition, the present study provided novel insight into the mechanisms of S1P actions in post-ischemic neovascularization, which includes the involvement of Akt/ERK-mediated eNOS activation and recruitment of BMDCs. These observations collectively show usefulness of PLGA-S1P for therapeutic neovascularization.

PLGAs have been widely studied for use as vehicles for sustained-release preparations because of their desirable biocompatible and biodegradable properties (Crotts and Park, 1998). In fact, injections of PLGA alone did not induce adverse tissue reactions in ischemic limbs or any abnormality in blood cell count, blood biochemistry and urinalysis in the present study. Several different methods have been proposed for synthesizing PLGA microspheres. Among these, the solvent diffusion method in water that we employed in the present study enabled one to generate PLGA microspheres with a favorable property: the PLGA microspheres synthesized by this method had the internal structure of a polymeric matrix containing dispersed drugs, giving continuous release of a drug (Kawashima et al., 1998). In the present study, we confirmed that S1P was continuously released from synthesized PLGA-S1P microparticles into the solution *in vitro* (see 2.4.). Repeated injections of the divided amounts over 28 days, rather than the single bolus injection, of PLGA-S1P microparticles conferred better results about stimulation of blood flow. This might have resulted from the fact that PLGA microspheres exhibit the initial burst of drug release and that higher local

concentrations of S1P in ischemic limbs than the optimal concentration do not effectively stimulate neovascularization as observed in our dose-response study of S1P solution injections (Oyama et al., 2008; Qi, X. unpublished results). The 3-day interval injections may have given the more favorable condition that permits an optimal range of local S1P concentration and its persistence. The particle size of PLGA microspheres could also affect release profile of drugs encapsulated in microspheres; smaller particles release more drugs per a given particle weight compared with larger particles because of the relatively greater surface area per weight in smaller particles (Kawashima et al., 1998). Therefore, it is possible that different sizes of PLGA microspheres show different dose-response relationships and optimal inter-injection time intervals even if they are made from an identical PLGA type.

The present study suggested that local injections of PLGA-S1P induced neovascularization at least through two ways, i.e. angiogenesis and recruitment of vascular mural cells, medial smooth muscle cells and pericytes (Fig. 4). Angiogenesis is the process in which new vessels arise by branching from existing microvessels, and involves the dissolution of the basement membrane underneath the endothelium, and EC migration and proliferation. Previous studies and our data suggest that S1P seems to stimulate angiogenesis through multiple mechanisms. First, S1P is capable of acting on ECs to stimulate endothelial proliferation, migration, cell-cell adhesion *in vitro*, and microvessel formation *in vivo* in matrices implanted in animals (Krump-Konvalinkova et al., 2008; Lee et al., 1999; Lee et al.,

2000; Ryu et al., 2002). Second, injections of PLGA-S1P increased the expression of several angiogenic factors including HGF, angiopoietin-1, SDF-1 and IL-1β in ischemic muscle (Fig. 5). Third, S1P recruited BMDCs, which release angiogenic growth factors and the powerful matrix-degrading enzymes matrix metalloproteinases, into ischemic muscle (Losordo and Dimmeler, 2004b; Ohki et al., 2005). With respect to this, in vitro activation of BMDCs via $S1P_3$ increased the capacity of the infused BMDCs to restore blood flow in ischemic limb (Walter et al., 2007). In that study, $S1P_3$ was suggested to be involved in homing of BMDCs through sensitization of SDF-1/CXCR4 signaling pathway. Therefore, the observed PLGA-S1P-induced increase in BMDCs in ischemic limb muscle (Fig. 8) may have been caused through $S1P_3$-SDF-1/CXCR4 pathway. These observations collectively suggest that exogenous S1P stimulates neovascularization by promoting angiogenesis through both EC-autonomous and non-autonomous mechanisms.

Injections of PLGA-S1P increased the number of αSMA-positive blood vessels in ischemic muscle (Fig. 4C middle), suggesting that S1P promoted smooth muscle-coverage of blood vessels, i.e. arteriogenesis. Arteriogenesis generally involves growth and remodeling of preexisting collateral vessels or reflects de novo formation of mature vessels (Carmeliet, 2000; Simons, 2005). The maturation of blood vessels into multilayer structure is essential for their persistence. In addition, we observed that PLGA-S1P promoted the association of pericytes with microvessels (Fig. 4B and 4C right), stabilizing newly formed vessels

(Carmeliet, 2000; Simons, 2005). The stabilization of capillaries probably inhibits regression of newly formed vessels and vascular permeability (Carmeliet, 2000; Simons, 2005). Previous studies (Allende et al., 2003; Choi et al., 2008; Liu et al., 2000; Paik et al., 2004) showed that S1P plays the essential role in mural cell recruitment at developmental vascular formation in an EC-autonomous manner. Therefore, it is the likely possibility that the vascular maturation effects of PLGA-S1P in ischemic limbs are mediated through S1P action on ECs. These stimulatory effects of S1P on angiogenesis and arteriogenesis may at least in part account for PLGA-S1P-induced increase in blood flow.

In the present study, we for the first time reported the evaluation of limb edema by taking serial CT images of the thigh of hindlimbs and calculating soft tissue volume of hindlimbs. This technique is non-invasive and can be repeatedly applied to the same animals so that one can follow the time course of edema. We detected transient edema due to femoral arteriectomy itself. As reported previously with other methods (Ferrara and Kerbel, 2005; Losordo and Dimmeler, 2004a; Simons, 2005; Takahashi and Shibuya, 2005), VEGF induced sustained edema after the surgery-induced initial edema (Fig. 3B). Importantly, injections of PLGA-S1P suppressed VEGF-induced edema in ischemic limbs, which was consistent with the vascular stabilizing (see above) and barrier-protecive actions (Lee et al., 2006; Peng et al., 2004; Singleton et al., 2005) of PLGA-S1P.

Injections of PLGA-S1P stimulated Akt and ERK in ischemic limb muscle (Fig. 6). Akt

and ERK are key signaling molecules in cell proliferation, survival, migration, eNOS activation in ECs, and thereby angiogenesis. In fact, injections of PLGA-S1P induced an increase in phosphorylation level of eNOS at Ser^{1177}, which is the Akt and ERK phosphorylation site critical for its activation. Available evidence (Losordo and Dimmeler, 2004b; Rubic et al., 1998; Ziche et al., 1997) suggest that the eNOS/NO pathway contributes to angiogenesis. Administration of the NOS inhibitor L-NAME reduced blood flow in both PLGA-S1P treated and PLGA treated control mice; PLGA-S1P still stimulated blood flow in L-NAME-administered mice (Fig. 7A), suggesting that mechanisms distinct from NO could also participate in PLGA-S1P-induced blood flow stimulation in ischemic limbs. Consistently, L-NAME tended to only partially inhibit PLGA-S1P-induced angiogenesis (Fig. 7B), suggesting that PLGA-S1P-induced neovascularization is in part dependent on eNOS/NO. These observations also suggest that NO may increase blood flow independently of stimulated neovascularization; NO-induced vasodilation may be involved in blood flow stimulation in ischemic limbs (Ziche et al., 1997). The eNOS/NO-independent angiogenic actions of PLGA-S1P likely involve Akt/ERK-mediated stimulation of endothelial cell proliferation and migration (Kimura et al., 2000; Lee et al., 1999; Ryu et al., 2002; Wang et al., 1999;). In addition, injections of PLGA-S1P partially rescued ischemia-induced limb necrosis (Fig. 2). Because both Akt and ERK act as the signaling pathways to mediate cell survival in various cell types including skeletal muscle (Woodgett, 2005), it is possible that S1P-induced

activation of Akt and ERK in skeletal muscle also contributed to protection of muscle from necrosis.

In conclusion, we developed PLGA-based slow release formulation of S1P for therapeutic angiogenesis. Repeated, local injections of the sustained release preparation promoted angiogenesis with stabilization and arteriogenesis through mechanisms involving Akt/ERK-eNOS and recruitment of BMDCs, resulting in stimulation of blood flow, prevention of necrosis and functional impairment without the adverse effects of local limb edema, bradycardia and lymphopenia. Thus, sustained delivery of S1P by topical injections of PLGA-S1P microspheres may represent a promising strategy for angiogenic therapy.

Acknowledgments

We thank C. Hirose and Y. Mishima for the secretarial assistance and the technical assistance, respectively. This work was supported by the Practical Application Research program of JST (Japan Science and Technology Agency) Innovation plaza Ishikawa and grants from the Ministry of Education, Science, Sports and Culture of Japan and the Japan Society for the Promotion of Science.

References

Allende, M.L., Yamashita, T., Proia, R.L., 2003. G-protein-coupled receptor S1P1 acts within endothelial cells to regulate vascular maturation. Blood 102, 3665–3667.

Allison, S.D., 2008. Effect of structural relaxation on the preparation and drug release behavior of poly(lactic-co-glycolic)acid microparticle drug delivery systems. J. Pharm. Sci. 97, 2022-2035.

Asahara, T., Masuda, H., Takahashi, T., Kalka, C., Pastore, C., Silver, M., Kearne, M., Magner, M., Isner, J,M., 1999. Bone marrow origin of endothelial progenitor cells responsible for postnatal vasculogenesis in physiological and pathological neovascularization. Circ. Res. 85, 221-228.

Carmeliet, P., 2000. Mechanisms of angiogenesis and arteriogenesis. Nat. Med. 6, 389-395.

Chae, S.S., Paik, J.H., Furneaux, H., Hla, T., 2004. Requirement for sphingosine-1- phosphate receptor-1 in tumor angiogenesis demonstrated by in vivo RNA interference. J. Clin. Invest. 114, 1082–1089.

Choi, J.W., Lee, C.W., Chun, J., 2008. Biological roles of lysophospholipid receptors revealed by genetic null mice: an update. Biochim. Biophys. Acta. 1781, 531-539.

Crotts, G., Park, T.G., 1998. Protein delivery from poly(lactic-co-glycolic acid) biodegradable microspheres: release kinetics and stability issues. J. Microencapsul. 15, 699-713.

Ferrara, N., Kerbel, R.S., 2005. Angiogenesis as a therapeutic target. Nature 438, 967–974.

Forrest, M., Sun, S.Y., Hajdu, R., Bergstrom, J., Card, D., Doherty, G., Hale, J., Keohane, C., Meyers, C., Milligan, J., Mills, S., Nomura, N., Rosen, H., Rosenbach, M., Shei, G.J., Singer, II., Tian, M., Wes,t S., White, V., Xie, J., Proia, R.L., Mandala, S., 2004. Immune cell regulation and cardiovascular effects of sphingosine 1-phosphate receptor agonists in rodents are mediated via distinct receptor subtypes. J Pharmacol. Exp. Ther. 309, 758-768.

Helisch, A., Wagner, S., Khan, N., Drinane, M., Wolfram, S., Heil, M., Ziegelhoeffer, T., Brandt, U., Pearlman, J.D., Swartz, H.M., Schaper, W., 2006. Impact of mouse strain differences in innate hindlimb collateral vasculature. Arterioscler. Thromb. Vasc. Biol. 26, 520-526.

Igarashi, J., Bernier, S.G., Michel, T., 2001. Sphingosine 1-phosphate and activation of endothelial nitric-oxide synthase. J. Biol. Chem. 276, 12420-12426.

Ishii, I., Fukushima, N., Ye, X., Chun, J., 2004. Lysophospholipid receptors: signaling and biology. Annu. Rev. Biochem. 73, 321-354.

Kawashima, Y., Yamamoto, H., Takeuchi, H., Hino, T., Niwa, T., 1998. Properties of a peptide containing DL-lactide/glycolide copolymer nanospheres prepared by novel emulsion solvent diffusion methods. Eur. J. Pharm. Biopharm. 45, 41-48.

Kimura, T., Watanabe, T., Sato, K., Kon, J., Tomura, H., Tamama, K., Kuwabara, A., Kanda, T., Kobayashi, I., Ohta, H., Ui, M., Okajima, F., 2000. Sphingosine 1-phosphate stimulates proliferation and migration of human endothelial cells possibly through the lipid receptors,

Edg-1 and Edg-3. Biochem. J. 348, 71-76.

Kluk, M.J., Hla, T., 2002. Signaling of sphingosine-1-phosphate via the S1P/EDG-family of G-protein-coupled receptors. Biochim. Biophys. Acta. 1582, 72–80.

Krump-Konvalinkova, V., Chwalla, I., Siess, W., 2008. FTY720 inhibits S1P-mediated endothelial healing: relationship to S1P1-receptor surface expression. Biochem. Biophys. Res. Commun. 370, 603-608.

Lee, J.F., Zeng, Q., Ozaki, H., Wang, L., Hand, A.R., Hla, T., Wang, E., Lee, M.J., 2006. Dual roles of tight junction-associated protein, zonula occludens-1, in sphingosine 1-phosphate-mediated endothelial chemotaxis and barrier integrity. J. Biol. Chem. 281, 29190-29200.

Lee, M.J., Thangada, S., Claffey, K.P., Ancellin, N., Liu, C.H., Kluk, M., Volpi, M., Shaafi, R.I., Hla, T., 1999. Vascular endothelial cell adherens junction assembly and morphogenesis induced by sphingosine-1-phosphate. Cell 99, 301–312.

Lee, O.H., Lee, D.J., Kim, Y.M., Kim, Y.S., Kwon, H.J., Kim, K.W., Kwon, Y.G., 2000. Sphingosine 1-phosphate stimulates tyrosine phosphorylation of focal adhesion kinase and chemotactic motility of endothelial cells via the G(i) protein-linked phospholipase C pathway. Biochem. Biophys. Res. Commun. 268, 47-53.

Liu, Y., Wada, R., Yamashita, T., Mi, Y., Deng, C.X., Hobson, J.P., Rosenfeldt, H.M., Nava, V.E., Chae, S.S., Lee, M.J., Liu, C.H., Hla, T., Spiegel, S., Proia, R.L., 2000. Edg-1,

G-protein-coupled receptor for sphingosine-1-phosphate, is essential for vascular maturation. J. Clin. Invest. 106, 951–961.

Losordo, D.W., Dimmeler, S., 20004a. Therapeutic angiogenesis and vasculogenesis for ischemic disease. Part I: angiogenic cytokines. Circulation 109, 2487–2491.

Losordo, D.W., Dimmeler, S., 2004b. Therapeutic angiogenesis and vasculogenesis for ischemic disease: part II: cell-based therapies. Circulation 109, 2692-2697.

Mizugishi, K., Yamashita, T., Olivera, A., Miller, G.F., Spiegel S., Proia, R.L., 2005. Essential role for sphingosine kinases in neural and vascular development. Mol. Cell. Biol. 25, 11113–11121.

Morris, A.J., Panchatcharam, M., Cheng, H.Y., Federico, L., Fulkerson, Z., Selim, S., Miriyala, S., Ecalante-Alcalde, D., Smyth, S.S., 2009. Regulation of blood and vascular cell function by bioactive lysophospholipids. J. Thromb. Haemost. Suppl. 1, 38-43.

Nofer, J.R., van der Giet, M., Tölle, M., Wolinska, I., von Wnuck Lipinski, K., Baba, H.A., Tietge, U.J., Gödecke, A., Ishii, I., Kleuser, B., Schäfers, M., Fobker, M., Zidek, W., Assmann, G., Chun, J., Levkau, B., 2004. HDL induces NO-dependent vasorelaxation via the lysophospholipid receptor S1P3. J. Clin. Invest. 113, 569–581.

Obst, M., Gross, V., Luft, F.C., 2004. Systemic hemodynamics in non-anesthetized L-NAME- and DOCA-salt-treated mice. J Hypertens. 22, 1889-1894.

Ohkawa, R., Nakamura, K., Okubo, S., Hosogaya, S., Ozaki, Y., Tozuka, M., Osima, N.,

Yokota, H., Ikeda, H., Yatomi, Y., 2008. Plasma sphingosine-1-phosphate measurement in healthy subjects: close correlation with red blood cell parameters. Ann. Clin. Biochem. 45, 356-363.

Ohki, Y., Heissig, B., Sato, Y., Akiyama, H., Zhu, Z., Hicklin, D.J., Shimada, K., Ogawa, H., Daida, H., Hattori, K., Ohsaka, A., 2005. Granulocyte colony-stimulating factor promotes neovascularization by releasing vascular endothelial growth factor from neutrophils. FASEB J. 19, 2005-7.

Oyama, O., Sugimoto, N., Qi, X., Takuwa, N., Mizugishi, K., Koizumi, J., Takuwa, Y., 2008. The lysophospholipid mediator sphingosine-1-phosphate promotes angiogenesis in vivo in ischaemic hindlimbs of mice. Cardiovascular. Res. 78, 301-307.

Paik, J.H., Skoura, A., Chae, S.S., Cowan, A.E., Han, D.K., Proia, R.L., Hla, T., 2004. Sphingosine 1-phosphate receptor regulation of N-cadherin mediates vascular stabilization. Genes Dev. 18, 2392-2403.

Peng, X., Hassoun, P.M., Sammani, S., McVerry, B.J., Burne, M.J., Rabb, H., Pearse, D., Tuder, R.M., Garcia, J.G., 2004. Protective effects of sphingosine 1-phosphate in murine endotoxin-induced inflammatory lung injury. Am. J. Respir. Crit. Care Med. 169, 1245–1251.

Rikitake, Y., Hirata, K., Kawashima, S., Ozaki, M., Takahashi, T., Ogawa, W., Inoue, N., Yokoyama, M., 2002. Involvement of endothelial nitric oxide in

sphingosine-1-phosphate-induced angiogenesis. Arterioscler. Thromb. Vasc. Biol. 22, 108–114.

Rubic, R.D., Shesely, E.G., Maeda, N., Smithies, O., Segal, S.S., Sessa, W.C., 1998. Direct evidence for the importance of endothelium-derived nitric oxide in vascular remodeling. J. Clin. Invest. 101, 731-736.

Ryu, Y., Takuwa, N., Sugimoto, N., Sakurada, S., Usui, S., Okamoto, H., Matsui, O., Takuwa, Y., 2002. Sphingosine-1-phosphate, a platelet-derived lysophospholipid mediator, negatively regulates cellular Rac activity and cell migration in vascular smooth muscle cells. Circ. Res. 90, 325–332.

Shireman, P.K., Quinones, M.P., 2005. Differential necrosis despite similar perfusion in mouse strains after ischemia. J. Surg. Res. 129, 242-250.

Simons, M., 2005. Angiogenesis: where do we stand now? Circulation 111, 1556–1566.

Singleton, P.A., Dudek, S.M., Chiang, E.T., Garcia, J.G., 2005. Regulation of sphingosine 1-phosphate-induced endothelial cytoskeletal rearrangement and barrier enhancement by S1P1 receptor, PI3 kinase, Tiam1/Rac1, and alpha-actinin. FASEB J. 19, 1646-1656.

Takahashi, H., Shibuya, M., 2005. The vascular endothelial growth factor (VEGF)/ VEGF receptor system and its role under physiological and pathological conditions. Clin. Sci. (Lond) 109, 227–241.

Takuwa, Y., Okamoto, Y., Yoshioka, K., Takuwa, N., 2008. Sphingosine-1-phosphate

signaling and biological activities in the cardiovascular system. Biochim. Biophys. Acta. 1781, 483-488.

Urano, T., Ito, Y., Akao, M., Sawa, T., Miyata, K., Tabata, M. Morisada, T., Hato, T., Yano, M., Kadomatsu, T., Yasunaga, K., Shibata, R., Murohara, T., Akaike, T., Tanihara, H., Suda, T., Oike, Y., 2008. Angiopoietin-related growth factor enhances blood flow via activation of the ERK1/2-eNOS-NO pathway in a mouse hind-limb ischemia model. Arterioscler. Thromb. Vasc. Biol. 28, 827-834.

Visentin, B., Vekich, J.A., Sibbald, B.J., Cavalli, A.L., Moreno, K.M., Matteo, R.G., Garland, W.A., Lu, Y., Yu, S., Hall, H.S., Kundra, V., Mills, G.B., Sabbadini, R.A., 2006. Validation of an anti-sphingosine-1-phosphate antibody as a potential therapeutic in reducing growth, invasion, and angiogenesis in multiple tumor lineages. Cancer Cell 9, 225–238.

Walter, D.H., Rochwalsky, U., Reinhold, J., Seeger, F., Aicher, A., Urbich, C., Spyridopoulos, I., Chun, J., Brinkmann, V., Keul, P., Levkau, B., Zeiher, A.M., Dimmeler, S., Haendeler, J., 2007. Sphingosine-1-phosphate stimulates the functional capacity of progenitor cells by activation of the CXCR4-dependent signaling pathway via the S1P3 receptor. Arterioscler. Thromb. Vasc. Biol. 27, 275-282.

Wang, F., Van Brocklyn, J.R., Hobson, J.P., Movafagh, S., Zukowska-Grojec, Z., Milstien, S., Spiegel, S., 1999. Sphingosine 1-phosphate stimulates cell migration through a G(i)-coupled cell surface receptor. Potential involvement in angiogenesis. J. Biol. Chem. 274,

35343-35350.

Woodgett, J.R., 2005. Recent advances in the protein kinase B signaling pathway. Curr. Opin. Cell Biol. 17, 150-157.

Ziche, M., Morbidelli, L., Choudhuri, R., Zhang, H.-T., Donnini, S., Granger, H.J,. Bicknell, R., 1997. Nitric oxide synthase lies downstream from vascular endothelial growth factor-induced but not basic fibroblast growth factor-induced angiogenesis. J. Clin. Invest. 99, 2625-2634.

Legends for Figures

Figure 1. Local PLGA-S1P injections enhance the blood flow recovery in C57BL/6 mice.

(A) Protocol of administration of PLGA-S1P microparticles. (B) Laser Doppler blood flow (LDBF) pseudocolour images, as determined with an LDBF analyser, in mice that received either PLGA-S1P (180 pmol total S1P) at single bolus, 6-day interval or 3-day interval or PLGA alone at 3-day interval on postoperative day 28. (C) Ischaemic/non-ischaemic limb LDBF ratio value in mice that received either PLGA-S1P (180 pmol total S1P) at various administration interval or PLGA alone at 3-day interval for 28 days. Data represent the mean ± S.E.M. (n = 8 mice per group). * P< 0.05, PLGA-S1P at 3-day interval versus the PLGA. (D) Ischaemic/non-ischaemic limb LDBF ratio value in mice that received either various doses of PLGA-S1P or PLGA alone at 3-day interval for 28 days. Data represent the mean ± S.E.M. (n = 8 mice per group). * P< 0.05, the 54 pmol PLGA-S1P treated mice versus the PLGA treated mice; § P< 0.05, the 18 pmol PLGA-S1P treated mice versus the PLGA treated mice; † P< 0.05, the 1.8 pmol PLGA-S1P treated mice versus the PLGA treated mice.

Figure 2. Local PLGA-S1P injections enhance the blood flow recovery (A), inhibit the tissue damage (B), and improve the functional recovery (C) of the limbs in Balb/c mice.

(A) Ischaemic/non-ischaemic limb LDBF ratio value in mice that received either PLGA-S1P (180 pmol total S1P) or PLGA alone at 3-day interval for 28 days. (B) Mean severity scores

for tissue necrosis. The severity of hind limb tissue necrosis was serially assessed after operation. (C) Spontaneous active use scores of left hindlimbs. The functional recovery of hind limb was serially assessed after operation. Data represent the mean ± S.E.M. (n = 15 mice per group). * P< 0.05 and ** P< 0.01 versus the PLGA treated mice.

Figure 3. Effects of either alone of PLGA-S1P and VEGF and the combination on blood flow recovery (A) and tissue edema (B, C) in C57BL/6 mice. Ischaemic/non-ischaemic limb LDBF ratio value (A) and ischemic/non-ischemic tissue volume evaluated by X-ray imaging analysis (B) in mice that received either PLGA-S1P (180 pmol total S1P) or PLGA alone at 3-day interval with or without daily injections of 56 ng VEGF for 28 days. Data represent the mean ± S.E.M. (n = 8 mice per group). In A: * P< 0.05, PLGA treated mice versus PLGA-S1P treated mice; § P< 0.05, PLGA treated mice versus PLGA plus VEGF treated mice; † P< 0.05, PLGA treated mice versus the PLGA-S1P plusVEGF treated mice. In B, * P< 0.05, the PLGA treated mice versus the PLGA plus VEGF treated mice. § P< 0.05, the PLGA plus VEGF treated mice versus the PLGA-S1P plus VEGF treated mice; † P< 0.05, the PLGA-S1P treated mice versus the PLGA with VEGF treated mice. (C) Representative X-ray images on postoperative day 28 are shown. R: right; L: left.

Figure 4. PLGA-S1P stimulates angiogenesis and arteriogenesis in C57BL/6 mice. A and

B, EC marker CD31 (red) and smooth muscle cell marker αSMA (A) and pericyte marker (B) were detected by double immunofluorescence (green) in the ischemic hindlimb of PLGA treated (upper panel) and PLGA-S1P treated (lower panel) mice. Representative immunofluorescence images of of either marker and merge images are shown. (C) CD31 positive microvessels, αSMA positive vessels, αSMA positive vascular area and NG2 positive microvessels were quantified by Image J software (NIH). Data represent the mean ± S.E.M. (n = 4 or 5 mice per group). * P< 0.05 and ** P< 0.01 versus the PLGA treated mice. Scale bar =100 μm.

Figure 5. mRNA expression of angiogenic factors in ischemic hindlimb muscle in C57BL/6 mice. mRNA expression levels of angiogenic factors in calf muscle from PLGA-S1P treated (stippled) and PLGA-treated (open) mice on postoperative day 3, 7, and 14 were determined by real-time PCR. GAPDH was used as an endogenous control. Data are expressed as the ratio of the values in ischemic over non-ischemic muscle and represent the mean ± S.E.M. (n = 5 or 6 mice per group). * P< 0.05, ischemic limb versus non-ischemic limb; § P< 0.05, the PLGA-S1P treated mice versus the PLGA treated mice.

Figure 6. Phosphorylation of Akt, ERK and eNOS in ischemic muscle following injections of PLGA-S1P or PLGA in C57BL/6 mice. Muscle tissue homogenates from

PLGA-S1P treated (filled) and PLGA-treated (open) mice on postoperative day 28 were subjected to Western blot using antibodies against phospho-Akt and total Akt (A), phospho-ERK and total ERK (B), and phospho-eNOS and total eNOS (C) as described in ”Materials and Methods”. Quantitative analyses of band densities are also shown. Data represent the mean ± S.E.M. (n = 5 mice per group). * P< 0.05, ** P< 0.01 versus the PLGA treated mice.

Figure 7. Effect of Nω-nitro-L-arginine methylester (L-NAME) on PLGA-S1P induced stimulation of blood flow recovery in C57BL/6 mice. (A) Ischaemic/non-ischaemic limb LDBF ratio value in mice of the 4 experimental groups; PLGA treated mice with or without L-NAME, PLGA-S1P treated mice with or without L-NAME. Data represent the mean ± S.E.M. (n = 8 mice per group). * P< 0.05, PLGA-S1P treated mice versus PLGA treated mice. § P< 0.05, PLGA-S1P treated mice versus PLGA-S1P with L-NAME treated mice; † P< 0.05, PLGA treated mice versus PLGA with L-NAME treated mice. (B) Immunohistochemical analysis of CD31 in ischemic hindlimbs of PLGA treated and PLGA-S1P treated mice with or without L-NAME. Shown are representative images (upper panel) from calf muscle on postoperative day 28. Quantitative analysis of CD31-positive microvessel density is also shown (lower panel). Data represent the mean ± S.E.M. (n = 5 mice per group).* P< 0.05. Scale bar =100 μm.

Figure 8. PLGA-S1P promotes bone marrow-derived cells (BMDCs) recruitment into the ischemic area in C57BL/6 mice. (A) GFP-positive cell recruitment into the ischemic area is promoted by PLGA-S1P. Ischemic calf muscle was excised on postoperative day 28 from C57BL/6J mice that had received transplantation of bone marrow (BM) cells from GFP-transgenic mice 4 weeks before the operation, and GFP-positive BMDCs in muscle were counted . B, C, and D, CD11b- (B), CD45- (C), or Gr-1-(D) positive cells recruitment into the ischemic area are promoted by PLGA-S1P. Sections of the calf muscle in PLGA treated and PLGA-S1P treated mice were probed with anti-CD11, anti-CD45, or anti-Gr-1 immunostaining, and CD11b-, CD45-, or Gr-1-positive cells were counted. Quantitative analyses of positive cell number are also shown. Data represent the mean ± S.E.M. (n = 6 mice per group). * P< 0.05, the PLGA-S1P treated mice versus the PLGA treated mice. Scale bar =50 μm

Table 1.

Effects of PLGA-S1P injectons on body weight, BP, heart rate, CBC, BUN, ALT, and urine test in mice

Treatment	Body weight (gram)	Systolic blood pressure (mmHg)	Heart rate (beats/min)	RBC ($x10^4$/μl)	WBC ($x10^2$/μl)	Plt ($x10^4$/μl)	lymphocyte (%)	BUN (mg/dL)	ALT (IU/L)	Urine test
PLGA	25.2±0.5	108.2±1.2	543±12	923±18	24±2.4	29±9	82±8	27±2	19±3	Normal
PLGA-S1P	25.4±0.3	107.1±3.8	565±23	948±8	23±2.4	41±20	82±5	25±1	16±4	Normal

RBC, red blood cell; WBC, white blood cell; Plt, platelet; BUN, blood urea nitrogen; ALT, alanine aminotransferase.

Wild-type C57BL/6J mice that received repeated injections of PLGA or PLGA-S1P into hindlimbs at 3-day interval for 28 days were analysed for the indicated items, as described in the Method section. The values are mean±S.E.M. (n=6 in each group). There was no significant difference in any of these parameters between PLGA-S1P-administered and control mice.

Figure 1
Click here to download high resolution image

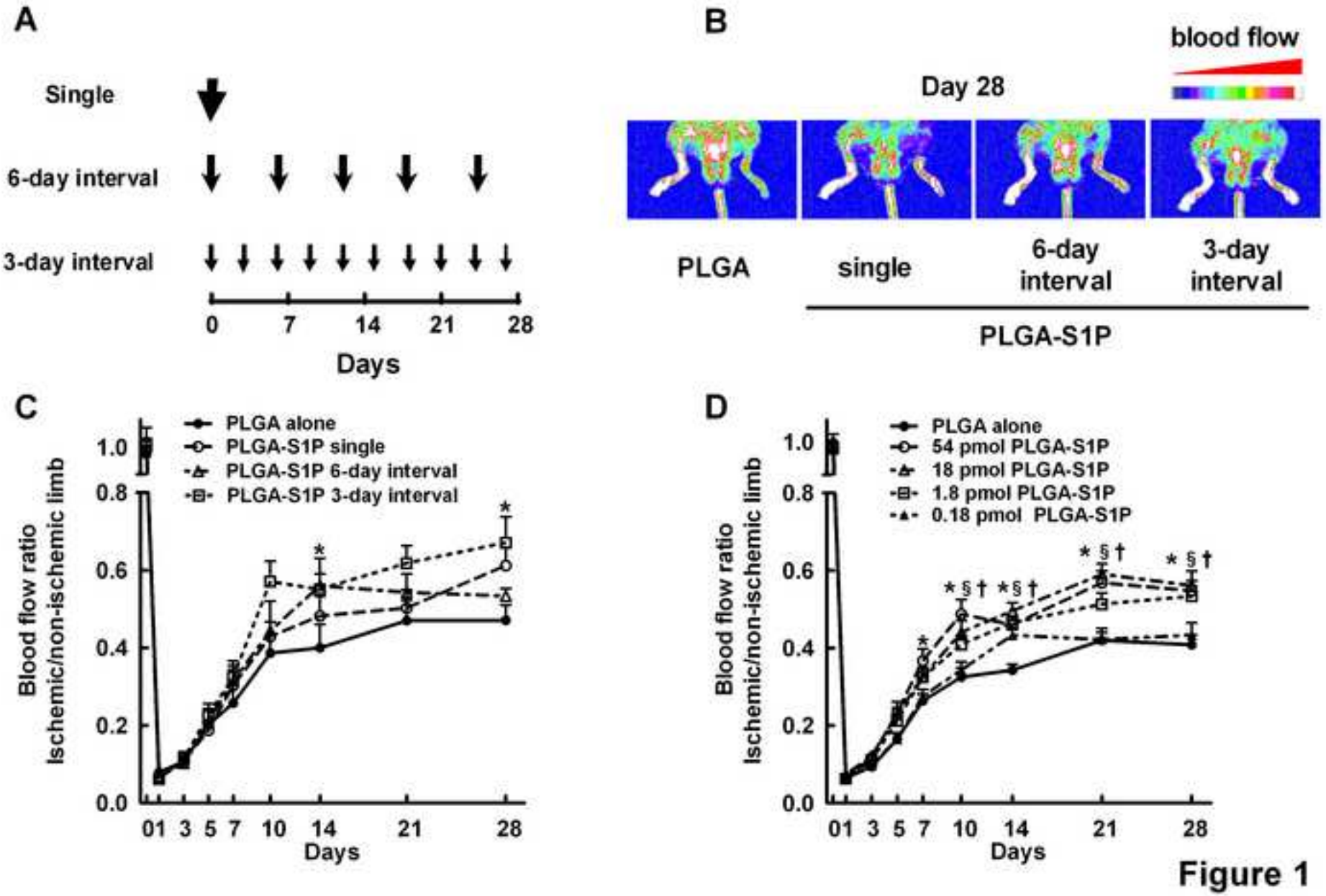

Figure 1

Figure 2

Click here to download high resolution image

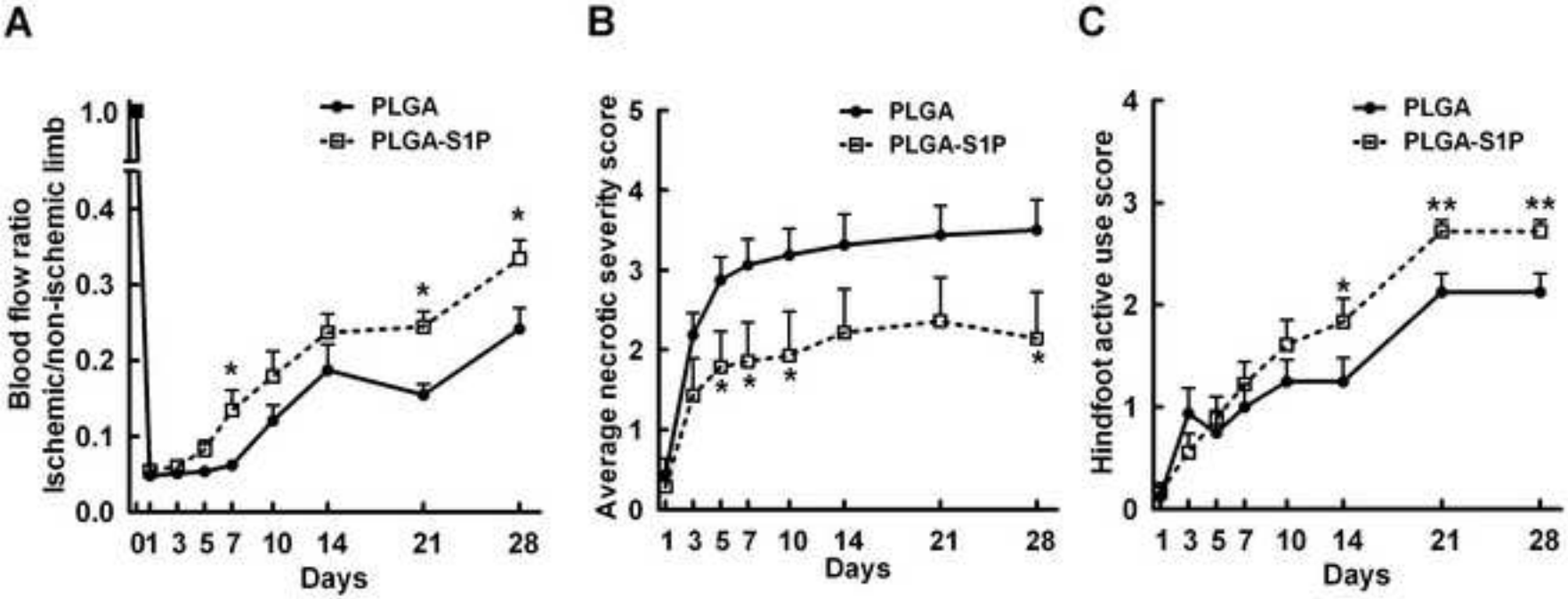

Figure 2

Figure 3
Click here to download high resolution image

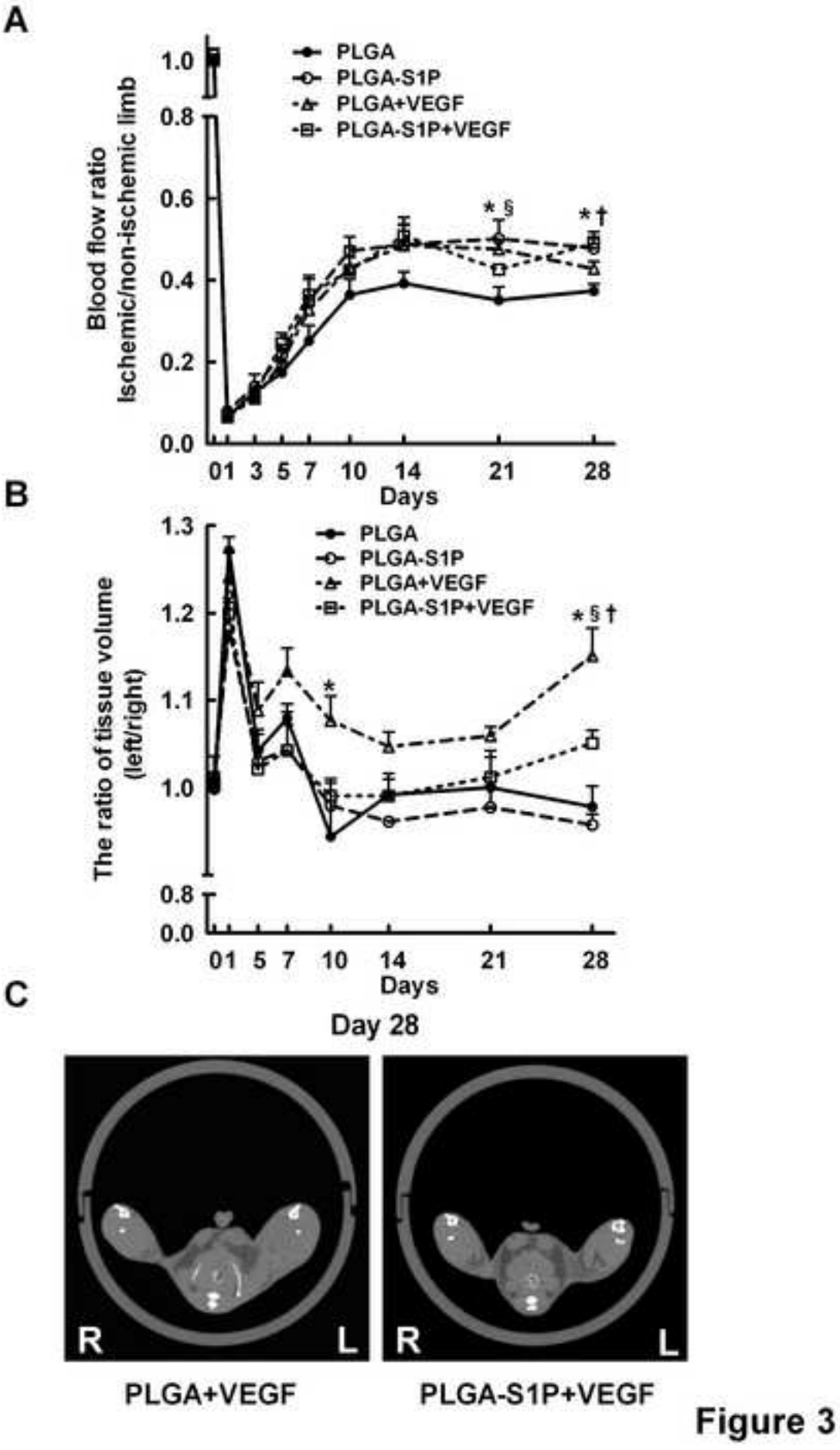

Figure 3

Figure?4

Click here to download high resolution image

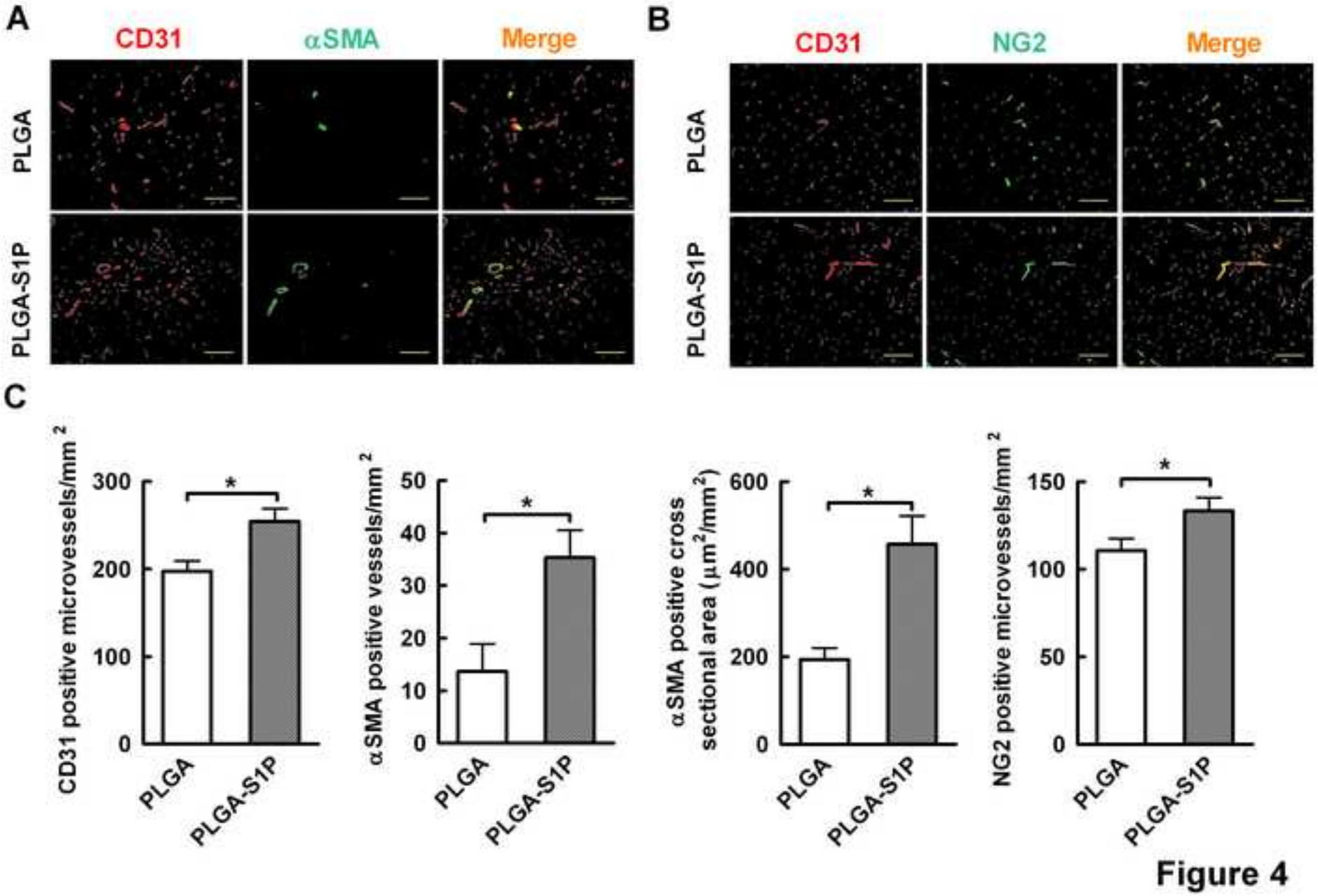

Figure 4

Figure 5
Click here to download high resolution image

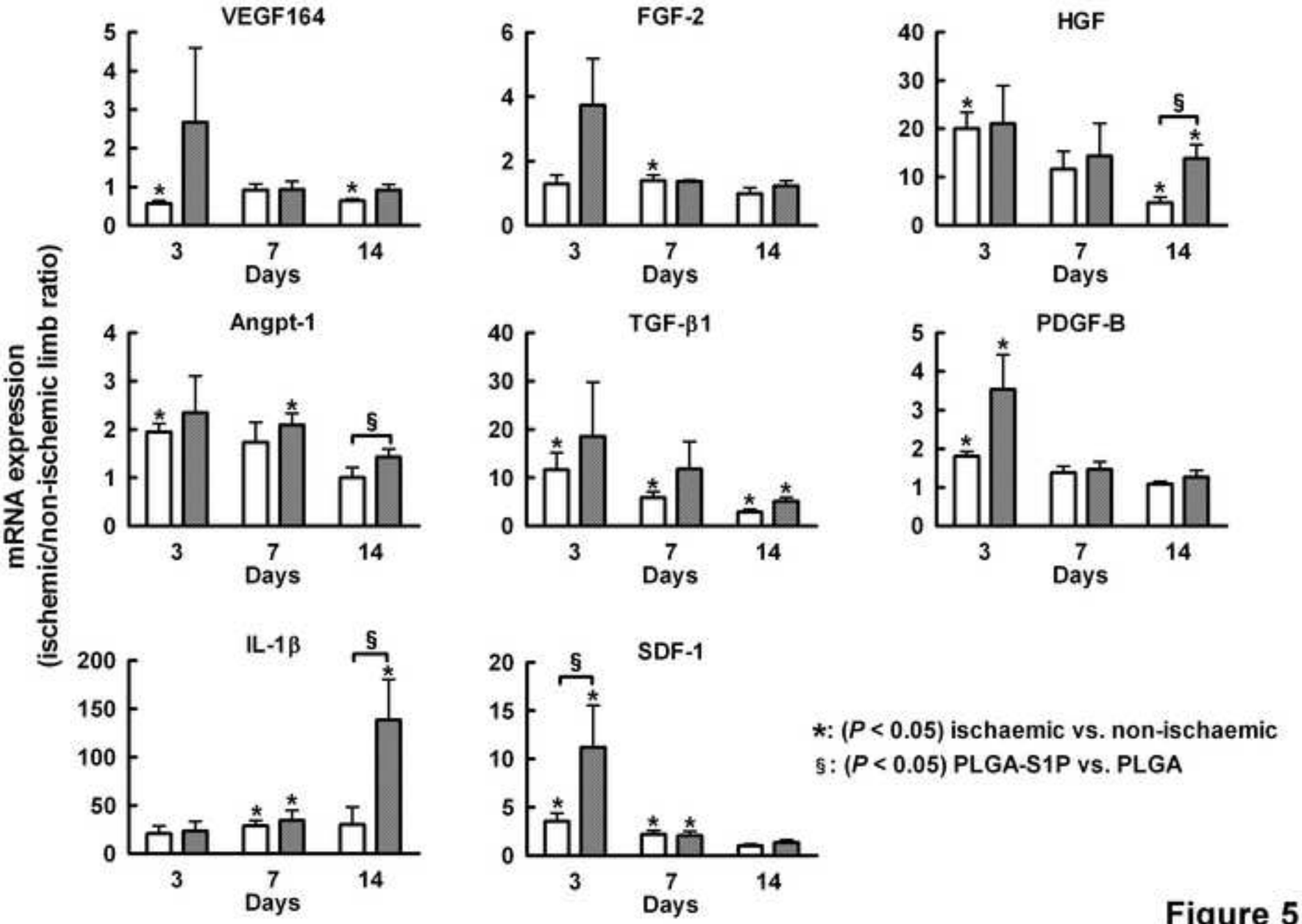

Figure 5

Figure 6

Click here to download high resolution image

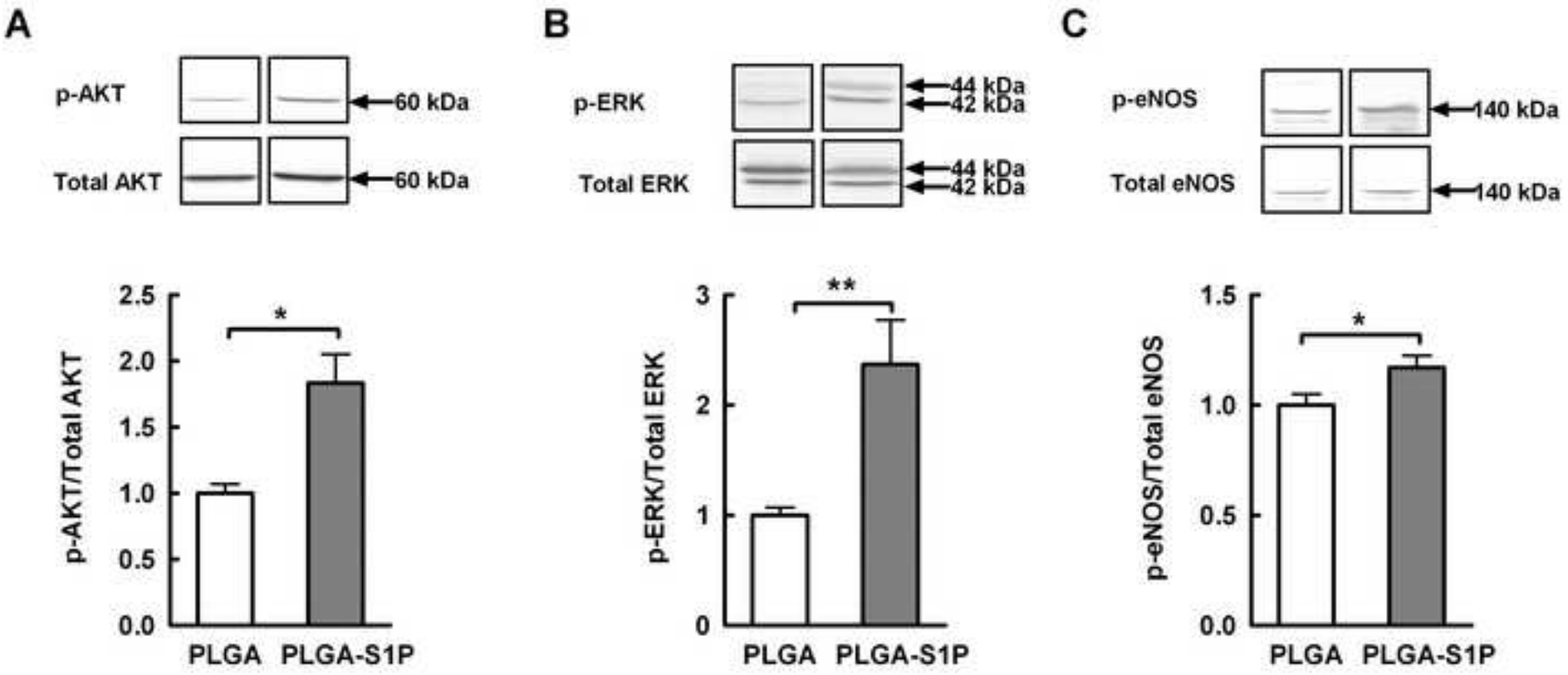

Figure 6

Figure 7
Click here to download high resolution image

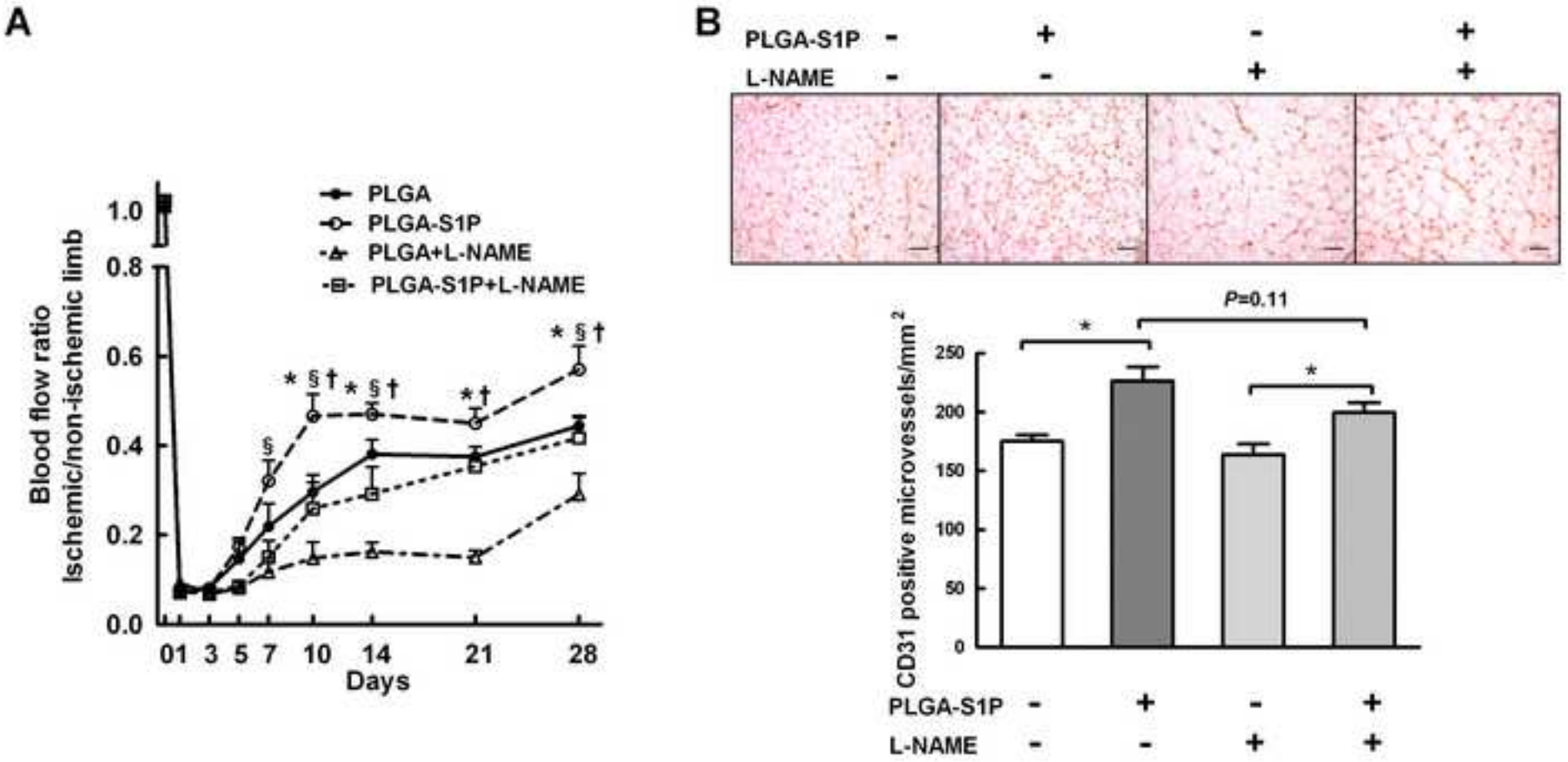

Figure 7

Figure 8
Click here to download high resolution image

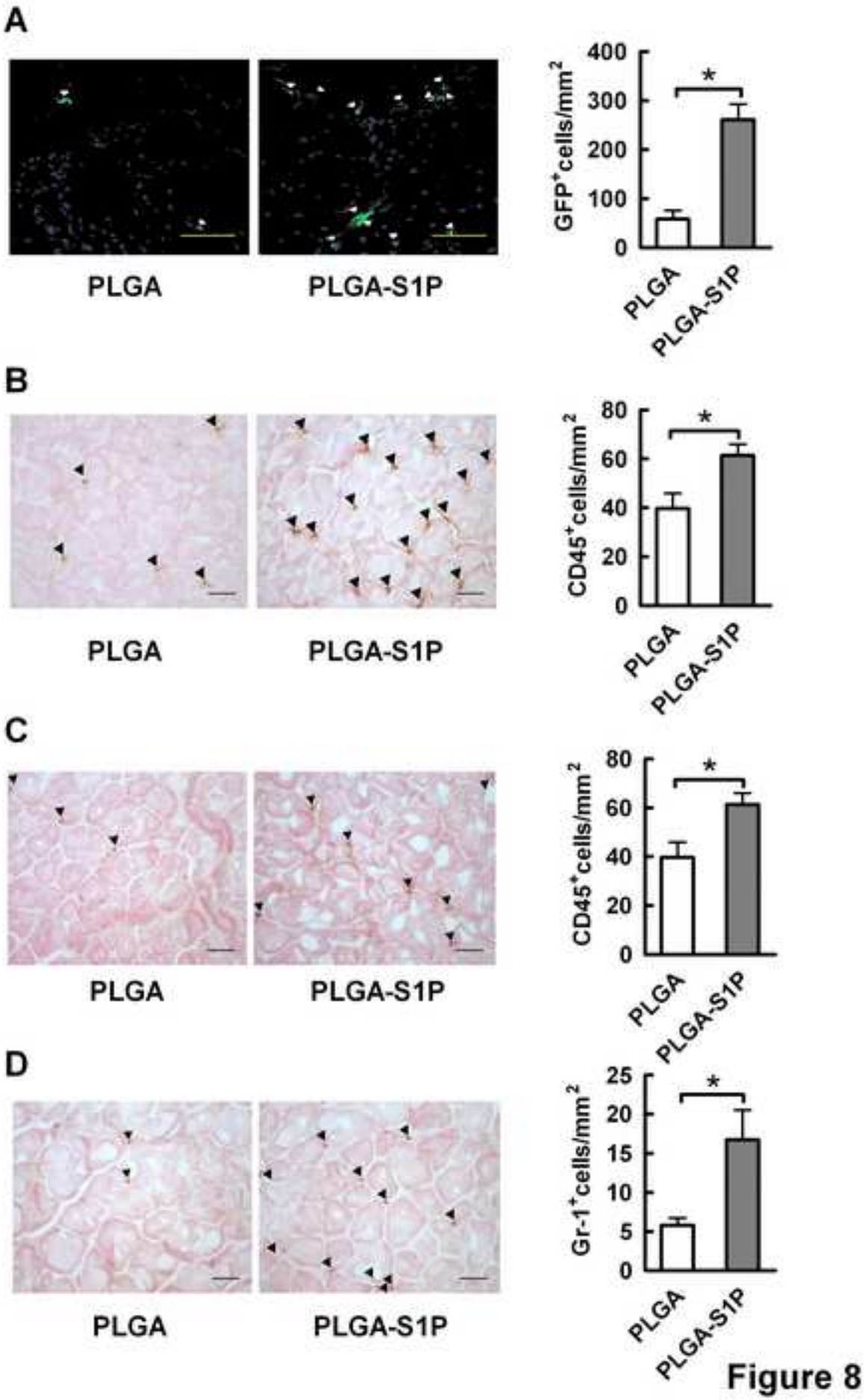

Figure 8